

Supporting Information

Contrasting decadal trends of subsurface excess nitrate in the western and eastern North Atlantic Ocean

Jin-Yu Terence Yang^{1,2}, Kitack Lee^{1*}, Jia-Zhong Zhang³, Ji-Young Moon¹, Joon-Soo Lee⁴, In-Seong Han⁴, Eunil Lee⁵

¹ Division of Environmental Sciences and Engineering, Pohang University of Science and Technology, Pohang 37673, Korea.

² State Key Laboratory of Marine Environmental Science, College of Ocean and Earth Sciences, Xiamen University, Xiamen 361102, China.

³ National Oceanic and Atmospheric Administration, Atlantic Oceanographic and Meteorological Laboratory, Miami, FL 33149, USA.

⁴ Ocean Climate and Ecology Research Division, National Institute of Fisheries Science, Busan 46083, Korea.

⁵ Ocean Research Division, Korea Hydrographic and Oceanographic Agency, Busan 49111, Korea.

***Corresponding author:**

Kitack Lee

Phone: +82-54-2792285; fax: +82-54-2798299; e-mail: ktl@postech.ac.kr

Files in the SI Appendix (1 text; 3 tables; 12 figures; 20 pages)

Text S1

Table S1 to S3

Figure S1 to S12

References

Text S1

Our analysis of NATl nutrient data was primarily focused on data obtained during the past 3 decades. Previous studies have also confirmed that during this period the physical (i.e., potential temperature and salinity) and chemical (i.e., nutrients and oxygen) properties of deep waters (> 2000 m depth) in the western and eastern subtropical NATl have not changed discernibly (Zhang et al., 2000; Gebbie and Huybers, 2012; Key et al., 2015; Olsen et al., 2016; Woosley et al., 2016). Moreover, we found no significant changes in salinity, potential temperature, and concentration of dissolved oxygen (DO) in the deep waters at the Bermuda Atlantic Time-series Study (BATS at 2000–3500 m depth) site in the western NATl and at the Iceland Sea Time-series site (68.0°N, 12.7°W; at 1500–1800 m depth) in the eastern NATl during the period 1990–2015 (Fig. S2).

The methods of nutrient and oxygen measurement in oceanography have been improved over time. The GO-SHIP program is an ongoing international repeat hydrography program and has provided the accurate oceanographic measurements using the most updated methodology (Talley et al., 2016). On each of the four transects the concentration profiles of nutrients and DO measured during the most recent cruises (the GO-SHIP program; Table S1) were used as the reference to correct the inaccuracy in historical data because of limitations in analytical technique and instrumentation used in early days. The differences (individual cruise data minus the GO-SHIP data) in concentrations of DIN, DIP, and DO in deep waters (where the concentration gradients were smallest) within a pixel of 1° (or 1.5°) latitude by 1.5° longitude were then calculated (Fig. S1b). For each pixel the estimated differences for all parameters along the density layers were finally applied to all cruise data other than the reference GO-SHIP data collected from the same pixel (Fig. S3). This data adjustment method would minimize systematic errors in data used in our analysis (Zhang et al., 2000).

Changes in nutrient concentrations associated with changes in remineralization (equivalent to changes in apparent oxygen utilization; AOU) were corrected using the DIP:DIN:O₂ remineralization ratio of 1:15:(-160) (Anderson and Sarmiento, 1994). We found no discernable effect of remineralization on any of the NATl deep water DIN_{xs} values, which is consistent with the results of previous studies (Broecker and Takahashi, 1980). For individual locations, multiplicative adjustment factors for nutrient concentrations were applied to the entire water column data if any differences were found in the deep waters (Key et al., 2015; Olsen et al., 2016).

Table S1. Detailed information of cruises and transects used in this study. Data collected in these cruises were shown in Figure 1.

| Program/ Data source | Expocode | Date | Extent | Nominal Lat./Long. |
|-------------------------|--------------|------------------|-------------|-----------------------|
| A22 | | | | |
| GEOSECS | GEOSECS_ATL | 3/30/1973 | 35°N–36°N | 67°W–68°W |
| TTO | 316N19810401 | 4/5–4/25/1981 | 18.5°N–36°N | 66°W |
| WOCE | 316N19970815 | 8/15–9/3/1997 | 18.5°N–36°N | 66°W |
| CLIVAR | 316N20031023 | 10/23–11/13/2003 | 18.5°N–36°N | 66°W |
| GO-SHIP | 33AT20120324 | 3/24–4/17/2012 | 18.5°N–36°N | 66°W |
| A20 | | | | |
| GEOSECS | GEOSECS_ATL | 9/20–9/28/1972 | 18°N–34°N | 50°W–54°W |
| NODC | 32OC19830501 | 5/1–5/17/1983 | 15°N–36°N | 52°W |
| WOCE | 316N19970717 | 7/17–8/10/1997 | 15°N–36°N | 52°W |
| CLIVAR | 316N20030922 | 9/22–10/23/2003 | 15°N–36°N | 52°W |
| GO-SHIP | 33AT20120419 | 4/19–5/1/2012 | 15°N–36°N | 52°W |
| A16N | | | | |
| WOCE | 32OC19880723 | 7/23–8/27/1988 | 20°N–64°N | 20°W–25°W |
| CLIVAR | 33RO20030604 | 6/4–8/1/2003 | 20°N–64°N | 20°W–25°W |
| GO-SHIP | 33RO20130803 | 8/13–9/9/2013 | 20°N–64°N | 20°W–25°W |
| A05 | | | | |
| WOCE | 33RO19980123 | 1/23–2/24/1998 | 75°W–14°W | 24.5°N |
| CLIVAR | 74DI20040404 | 4/4–5/10/2004 | 75°W–14°W | 24.5°N |
| GO-SHIP | 74DI20100106 | 1/6–2/18/2010 | 75°W–14°W | 24.5°N |

Table S2. Overall average adjustment factors (%) obtained from comparisons of the nutrients (DIN and DIP) concentrations for the deep water along the four transects at crossover stations. The comparison data were taken from the depths with minimum concentration gradients. The latest GO-SHIP cruises (see Table S1) were used as the reference against which historical cruises were compared. The average adjustment factors for the DIN and DIP are consistent to those in the GLODAPv2 product (Olsen et al., 2016).

| Transect/ Cruise year | Average adjustment factor (%) | |
|--------------------------|-------------------------------|------------|
| | DIN | DIP |
| A22 | | |
| 1997 | 0.75±0.57 | 0.21±0.46 |
| 2003 | -0.47±0.90 | -1.54±0.60 |
| A20 | | |
| 1983 | -0.39±1.01 | -0.71±1.48 |
| 1997 | -0.07±0.63 | -0.44±0.57 |
| 2003 | -0.17±0.76 | -0.78±0.76 |
| A16N | | |
| 1988 | 0.50±1.56 | -4.03±3.00 |
| 2003 | -0.02±1.60 | -1.31±1.99 |
| A05 | | |
| 1998 | 0.14±1.68 | 1.05±1.79 |
| 2004 | 0.63±3.41 | 0.02±3.29 |

Table S3. Locations of monitoring sites of atmospheric wet nitrogen deposition along the US Atlantic coast. Annual average data of total inorganic nitrogen deposition were derived from the sites with an observation period were greater than 15 years. Data are available at <http://nadp.sws.uiuc.edu/>.

| Site ID | Latitude (°N) | Longitude (°W) | Observational Period |
|---------|---------------|----------------|----------------------|
| FL03 | 29.9748 | 82.1978 | 1978–2016 |
| FL05 | 28.7486 | 82.5551 | 1996–2016 |
| FL11 | 25.3900 | 80.6800 | 1980–2016 |
| FL41 | 27.3801 | 82.2831 | 1983–2016 |
| FL99 | 28.5428 | 80.6440 | 1983–2015 |
| GA09 | 30.7404 | 82.1283 | 1997–2016 |
| GA20 | 32.0849 | 81.9367 | 1983–2016 |
| MA01 | 41.9759 | 70.0241 | 1981–2016 |
| ME96 | 43.8325 | 70.0645 | 1998–2016 |
| ME98 | 44.3772 | 68.2608 | 1981–2016 |
| NC03 | 36.1325 | 77.1708 | 1978–2016 |
| NJ00 | 39.4728 | 74.4369 | 1998–2016 |
| PR20 | 18.3206 | 65.8200 | 1985–2016 |

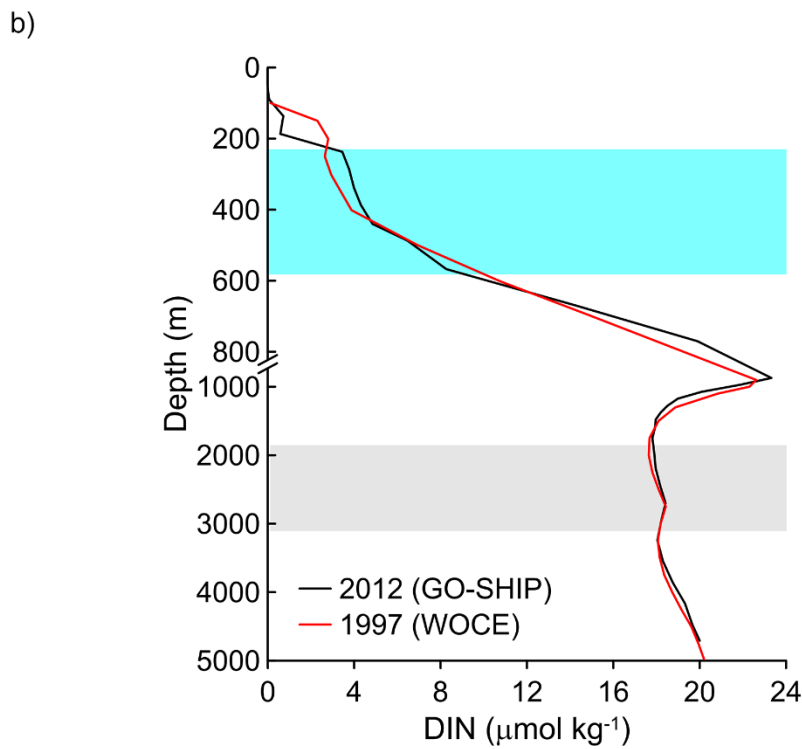
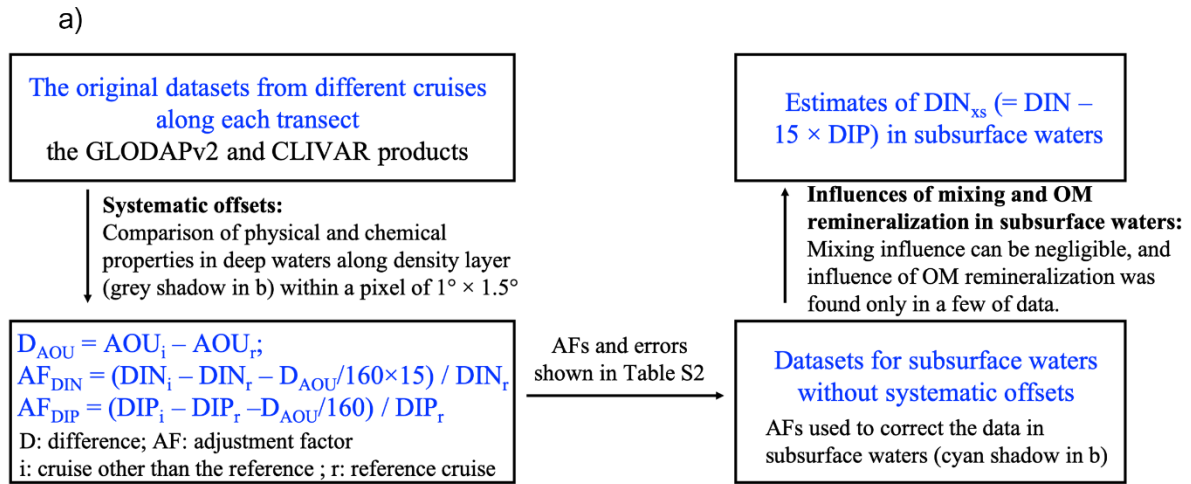
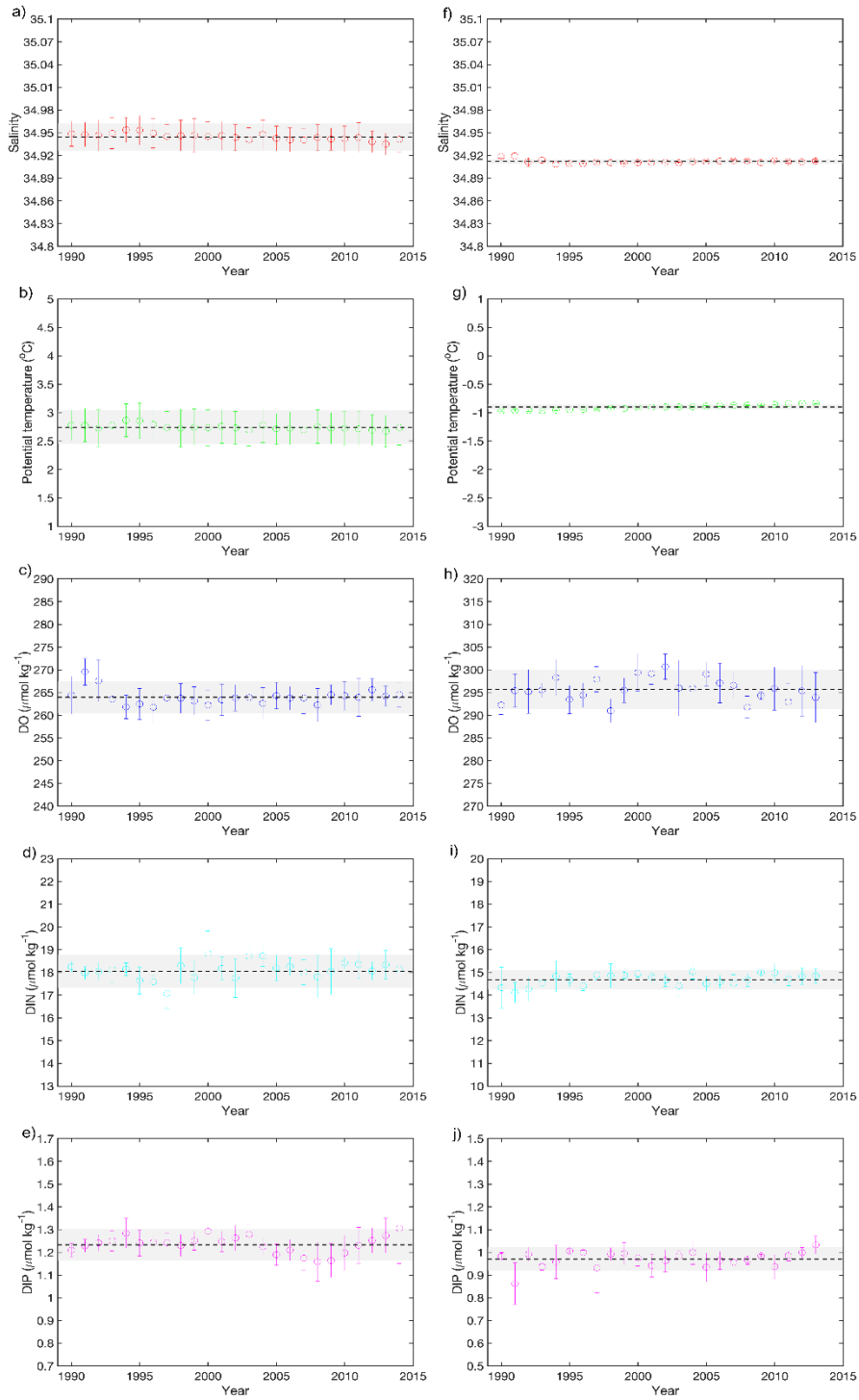


Figure S1. (a) Flow chart of the procedure used to adjust the original data from the GLODAPv2 product and CLIVAR database. (b) Example profile of DIN illustrating the adjustment methods. The main adjustments were derived from an examination of the systematic offsets that are shown in Table S2.



88

89 **Figure S2.** Temporal variations in salinity, potential temperature, and concentrations of
 90 dissolved oxygen (DO), DIN and DIP for the deep waters at the Bermuda Atlantic Time-
 91 series Study (BATS, 31.7°N, 64.2°W) site from 1990–2015 (a–e, 2000–3500 m) and a time-
 92 series site (68.0°N, 12.7°W) from 1990–2013 (f–j, 1500–1800 m) in the northern Iceland Sea.
 93 Data from BATS are derived from <http://bats.bios.edu/bats-data/>, while data from the Iceland
 94 Sea are from the Ocean Carbon Data System, NOAA
 95 (https://www.nodc.noaa.gov/ocads/oceans/Moorings/Iceland_Sea.html).
 96

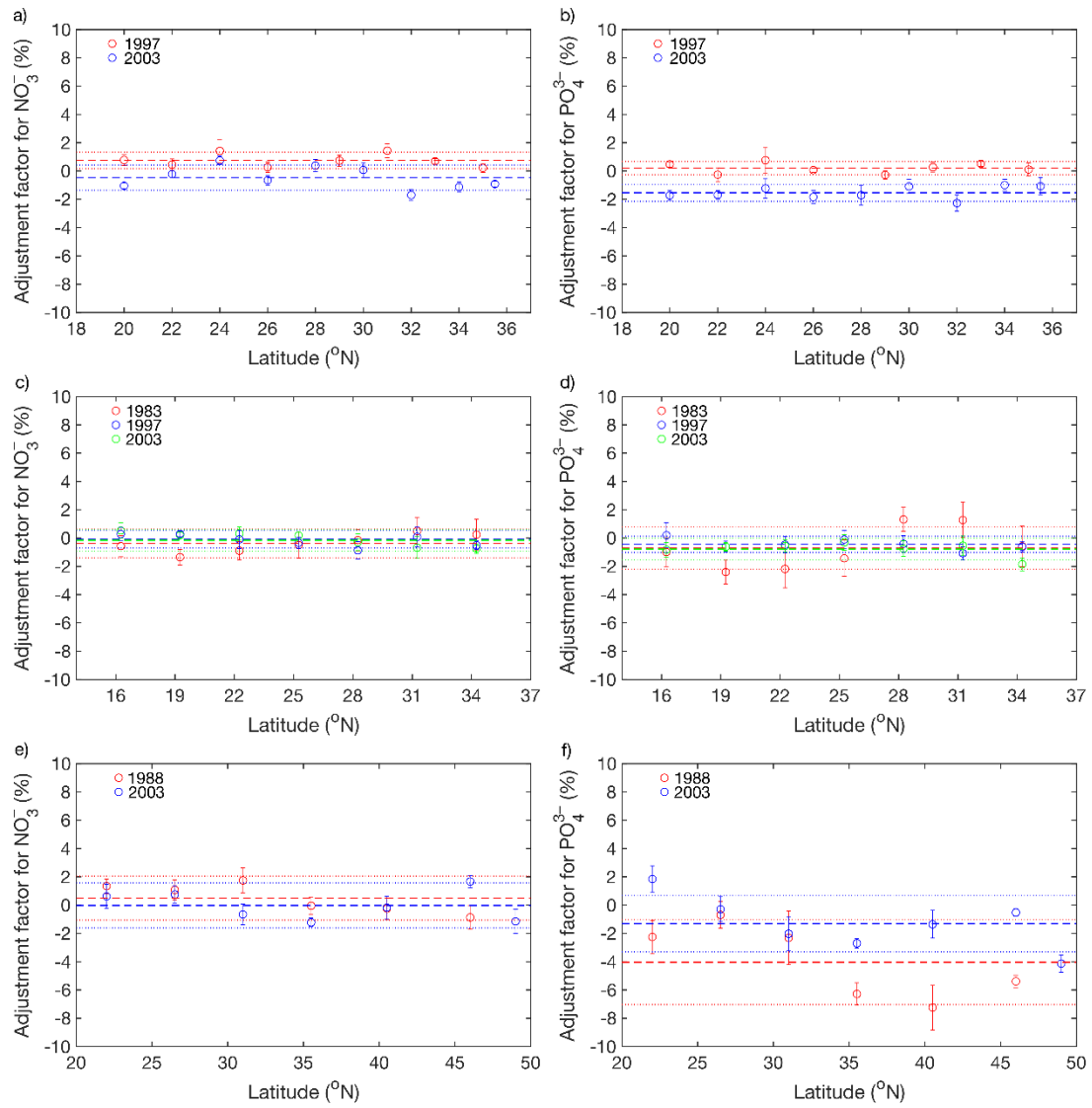


Figure S3. Adjustment factors of NO_3^- and PO_4^{3-} for the major cruises along A22 (a and b), A20 (c and d) and A16N (e and f) by 3° – 5° latitude. Data from the latest GO-SHIP cruise along each transect were used as references. The adjustment factors were obtained by comparing the deep-water parameters of different cruises with the reference data. The relatively high adjustment factors obtained for A16N are a result of the use of raw data rather than data from the GLODAPv2 product, because the latest cruise along A16N in 2013 is not included in the GLODAPv2 product.

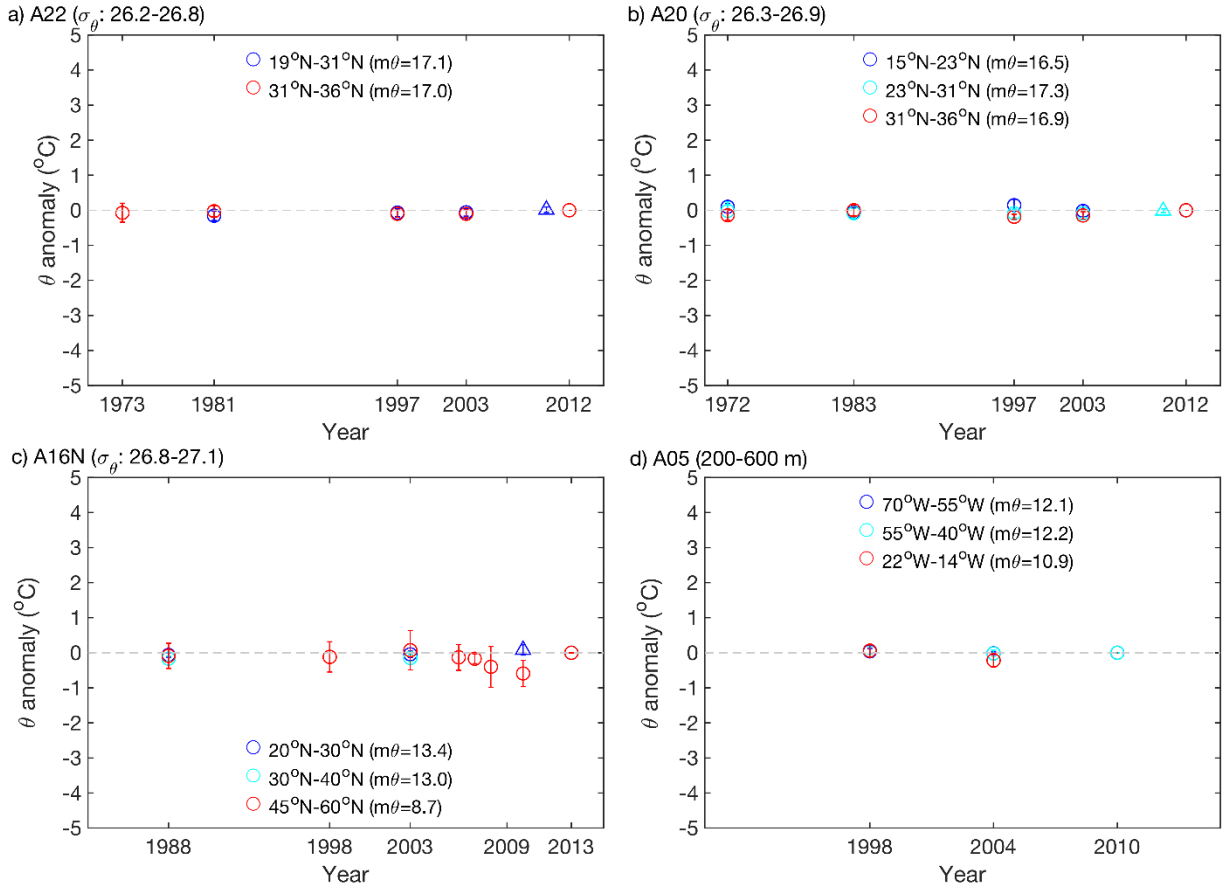


Figure S4. Temporal trends of potential temperature (θ) anomalies (dots) for the corresponding latitude or longitude intervals for the subsurface potential density intervals σ_θ along the four transects (a) A22, (b), (c) A16N (note that $\sigma_\theta = 27.2\text{--}27.6$ for the latitude interval of $45^\circ\text{N}\text{--}60^\circ\text{N}$), and (d) A05 in the NATl. The date from A05 obtained in 2010 at three crossover sites are also shown in a-c (triangles). θ anomalies indicate θ values minus the mean θ value in the GO-SHIP dataset ($m\theta$, values shown in parentheses). The selected density intervals are typically located at a water depth of 200–600 m, which encompasses the DIN_{xs} maximum. The selected σ_θ intervals in the subpolar region along A16N and in the eastern basin along A05 were different, as σ_θ for 200–600 m depth becomes larger in the high-latitude region or eastern basin. The gray dashed line indicates a θ anomaly of zero. The θ of a water mass occupying any given density surface did not change between repeat occupations (Student's t-test and ANOVA with Games-Howell test, $p > 0.05$) along the four transects in the NATl, except for a slight decrease in the subpolar region along A16N since the 2000s.

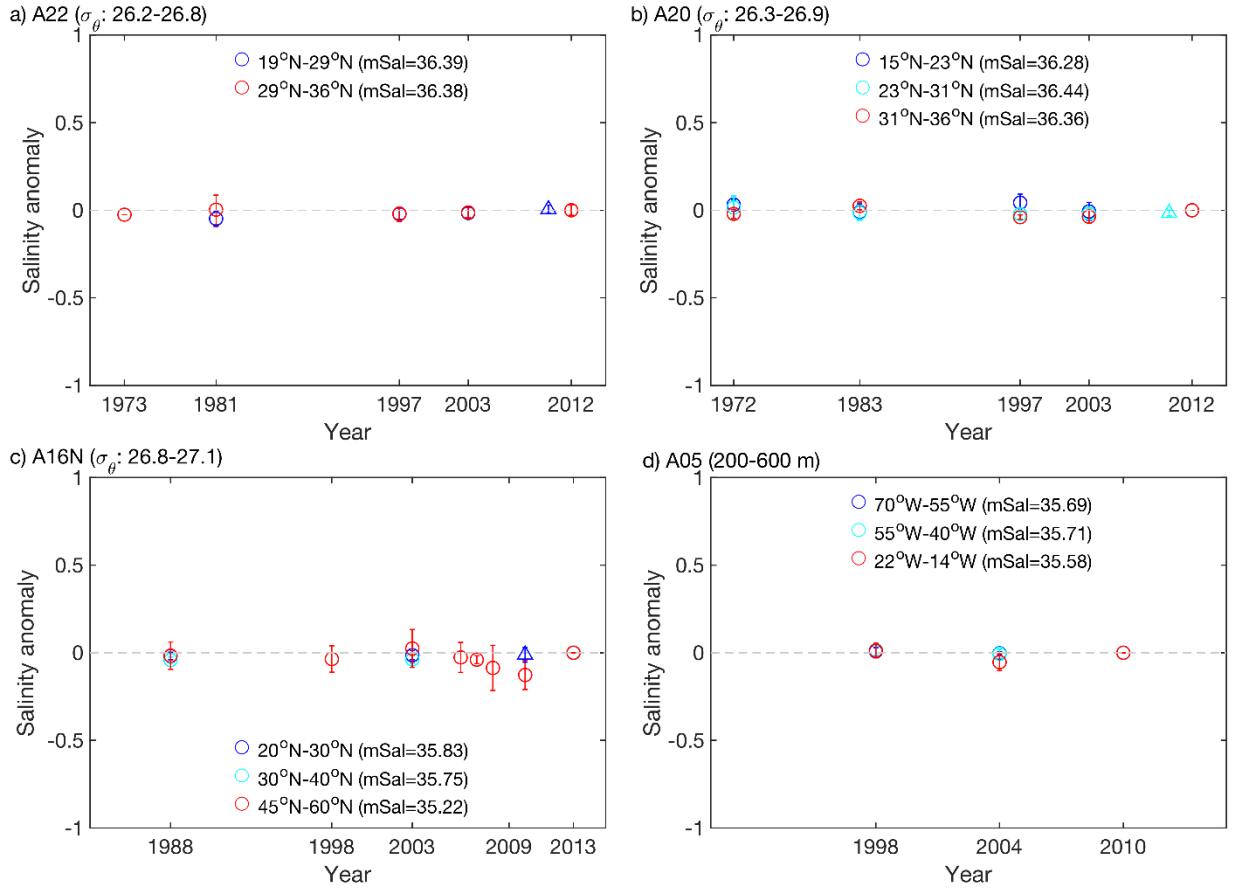


Figure S5. The same as in Figure S3 except for salinity anomalies. Salinity anomalies indicate salinity minus the mean value salinity in GO-SHIP dataset (mSal, their values in parentheses). The gray dashed lines indicate salinity anomaly of zero. The salinity of a water mass occupying any given density surface did not change between repeat occupations (Student's t-test and ANOVA with Games-Howell test, $p > 0.05$) along the four transects in the NATl, except for a slight decrease in the subpolar region along A16N since the 2000s.

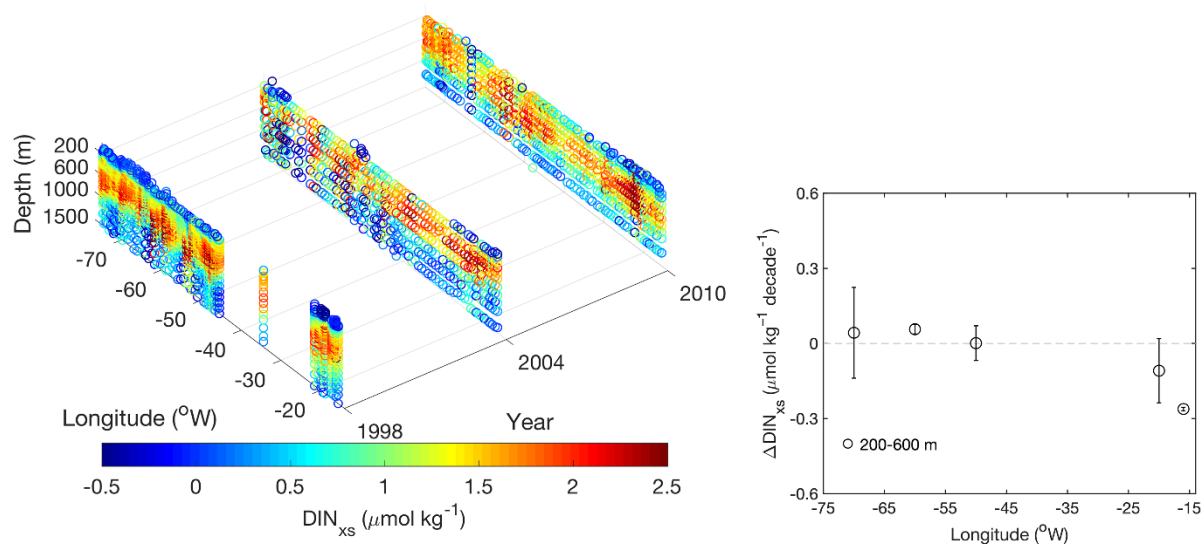


Figure S6. The vertical distributions of excess nitrate (DIN_{xs}) in the upper 1500 m for the difference cruises along the transect A05 in the NATl. The inset shows the average rates (with 95% confidence limits) of change in DIN_{xs} ($\Delta\text{DIN}_{\text{xs}}$) at 200–600 m averaged for each 6° – 10° longitude interval between GO-SHIP and WOCE time periods.

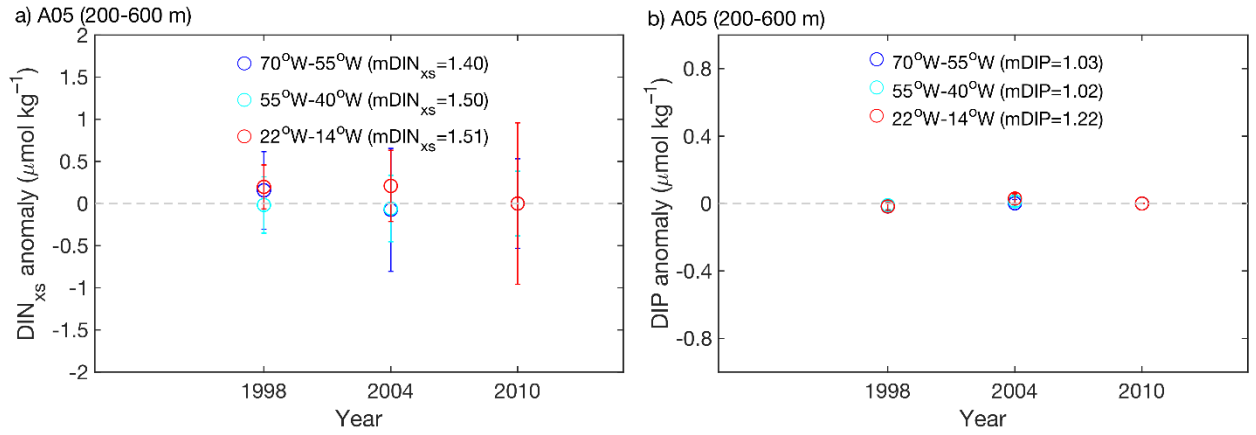


Figure S7. Temporal trends of DIN_{xs} (a) and DIP (b) anomalies for the corresponding longitude intervals for the subsurface potential density intervals σ_θ along A05 (see Fig. S2 caption) in the NATl. DIN_{xs} and DIP anomalies indicate DIN_{xs} and DIP concentrations minus the mean DIN_{xs} and DIP in GO-SHIP dataset (mDIN_{xs} and mDIP, their values in parentheses), respectively. The DIN_{xs} and DIP values were corrected by the changes in AOU (see text). The gray dashed lines in (a) and (b) indicate the DIN_{xs} and DIP anomalies of zero.

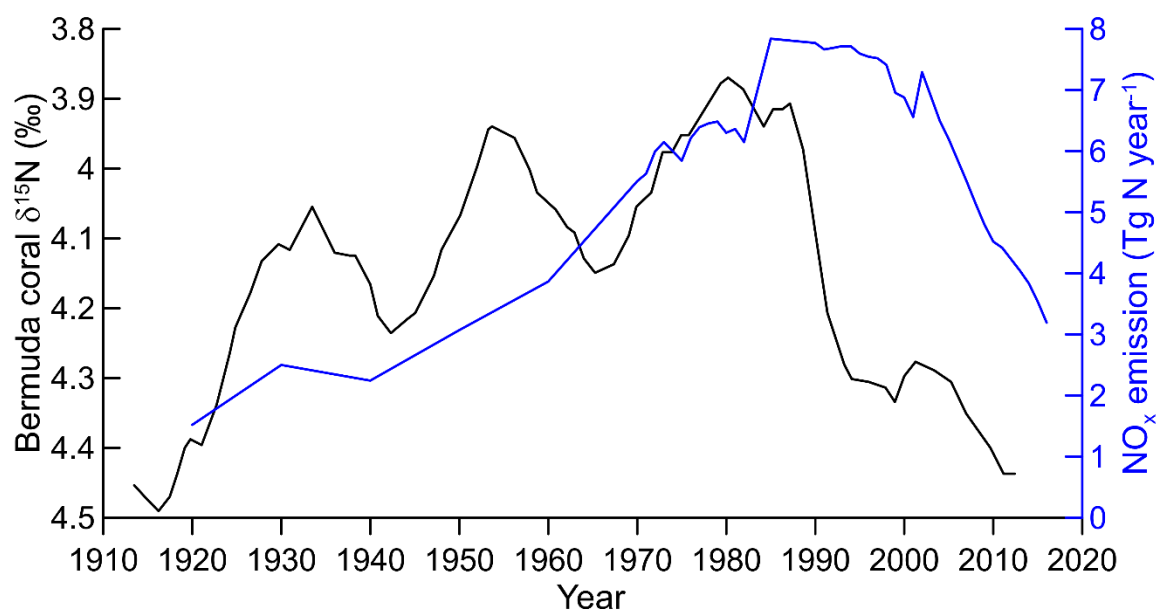


Figure S8. Temporal variations of Bermuda coral $\delta^{15}\text{N}$ (black; Wang et al., 2018) and NO_x emissions from the USA (blue; EPA, 2000).

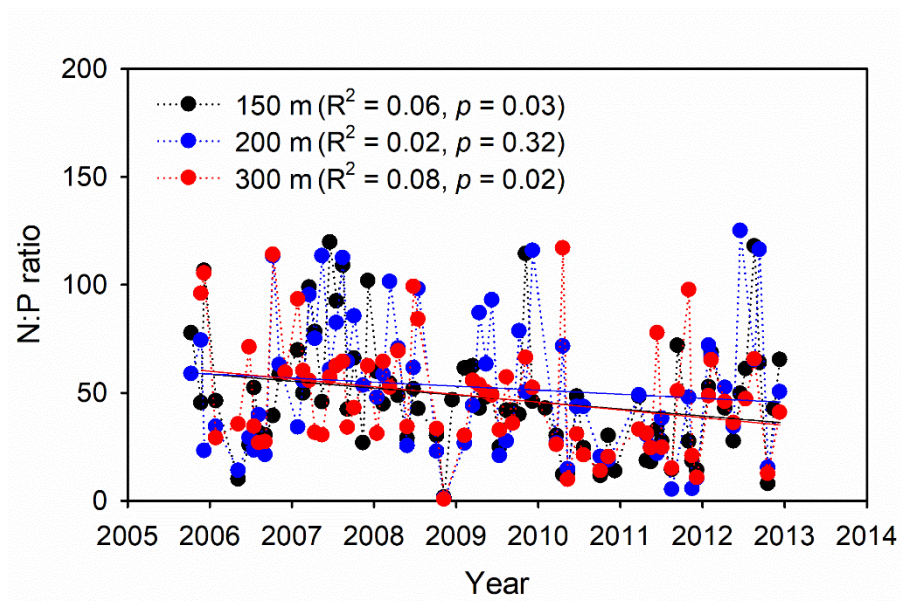


Figure S9. Temporal variations in the N:P ratios in sinking particles collected between 150 and 300 m at the BATS site.

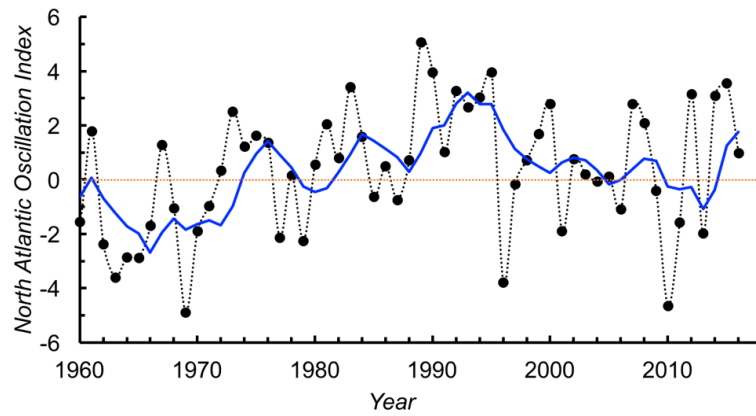


Figure S10. Temporal variation of the winter North Atlantic Oscillation index (solid dots). The blue curve shows the trend of 5-year moving average. Data are derived from the Climate and Global Dynamics division at National Centre for Atmospheric Research (<http://www.cgd.ucar.edu/cas/catalog/climind/>)

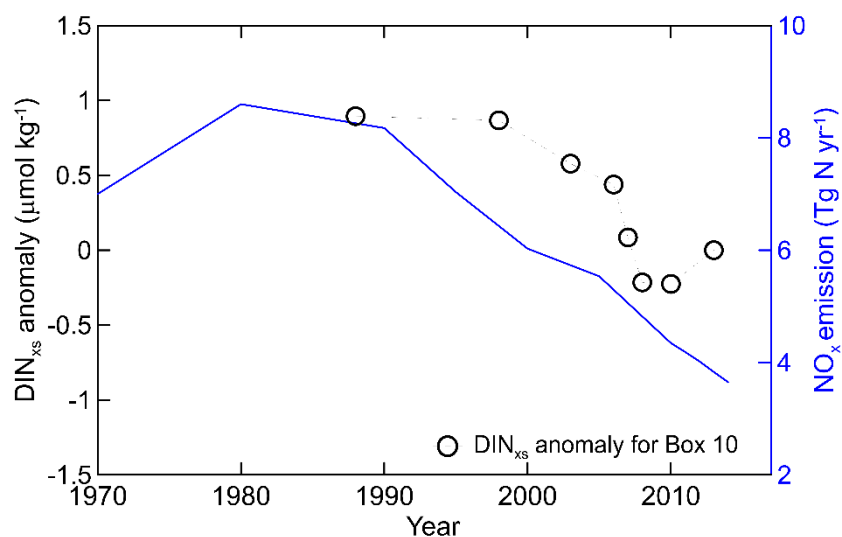


Figure S11. Temporal variations in DIN_{xs} anomaly in the subpolar region of the eastern North Atlantic where DIN_{xs} decreased significantly (box 10 in Figure 4a). The history of NO_x emissions from Europe (blue curve) is also shown (Adams et al., 2012).

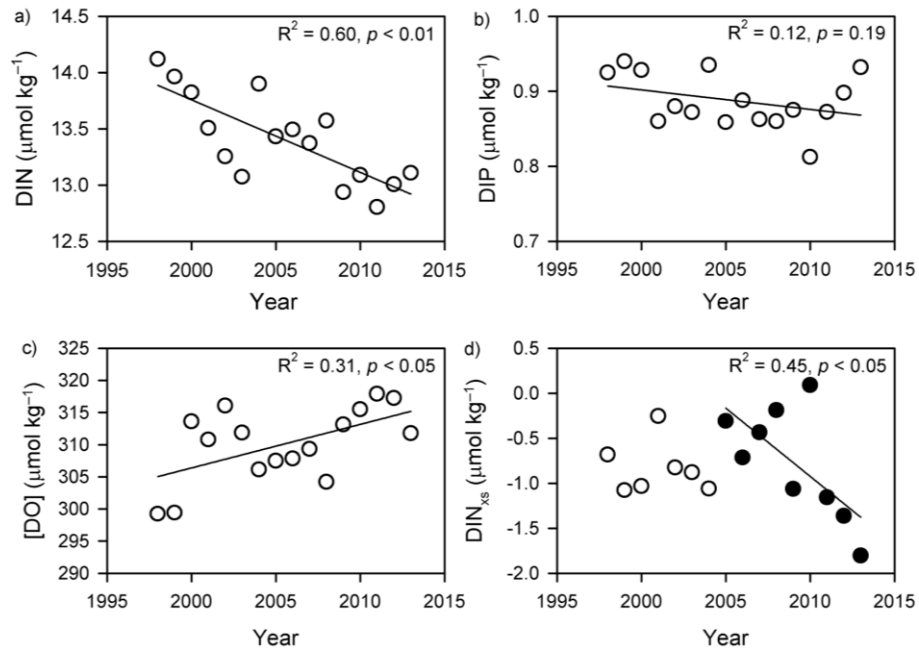


Figure S12. Temporal variations of annual average concentrations of (a) DIN, (b) DIP, (c) dissolved oxygen (DO) and (d) DIN_{xs} in the subsurface waters (300–500 m, potential density σ_θ of ~28.0) at a time series site (68.0°N, 12.7°W) from 1998–2013 in the northern Iceland Sea. Note that the linear regression in d) only include the data since the decreasing trend is significant after 2005. Data are derived from the Ocean Carbon Data System, NOAA (https://www.nodc.noaa.gov/ocads/oceans/Moorings/Iceland_Sea.html)

References

- Adams, M., Aardenne, J. V., Kampel, E., Tista, M., and Zuber A.: European Union emission inventory report 1990–2010 under the UNECE Convention on Long-range Transboundary Air Pollution (LRTAP), Eur. Environ. Agency, Copenhagen, <http://doi.org/10.2800/5219>, 2012.
- Anderson, L. A., and Sarmiento, J. L.: Redfield ratios of remineralization determined by nutrient data analysis, *Global Biogeochem. Cycles*, 8, 65-80, <http://doi.org/10.1029/93GB03318>, 1994.
- Broecker, W. S., and Takahashi, T.: Hydrography of the central Atlantic—III. The North Atlantic deep-water complex, *Deep Sea Res. Part A*, 27, 591-613, [http://doi.org/10.1016/0198-0149\(80\)90076-X](http://doi.org/10.1016/0198-0149(80)90076-X), 1980.
- EPA: National Air Pollutant Emission Trends, 1900–1998, Office of Air Quality Planning and Standards, Research Triangle Park, 2000.
- Gebbie, G., and Huybers, P.: The mean age of ocean waters inferred from radiocarbon observations: Sensitivity to surface sources and accounting for mixing histories, *J. Phys. Oceanogr.*, 42, 291-305, <http://doi.org/10.1175/jpo-d-11-043.1>, 2012.
- Key, R. M., Olsen, A., van Heuven, S., Lauvset, S. K., Velo, A., Lin, X., Schirnick, C., Kozyr, A., Tanhua, T., Hoppema, M., Jutterström, S., Steinfeldt, R., Jeansson, E., Ishii, M., Perez, F. F., and Suzuki, T.: Global Ocean Data Analysis Project, Version 2 (GLODAPv2), (ORNL/CDIAC-162, ND-P093), Carbon Dioxide Information Analysis Center, Oak Ridge National Laboratory, US Department of Energy, 2015.
- Olsen, A., Key, R. M., van Heuven, S., Lauvset, S. K., Velo, A., Lin, X., Schirnick, C., Kozyr, A., Tanhua, T., Hoppema, M., Jutterström, S., Steinfeldt, R., Jeansson, E., Ishii, M., Pérez, F. F., and Suzuki, T.: The Global Ocean Data Analysis Project version 2 (GLODAPv2) – an internally consistent data product for the world ocean, *Earth Syst. Sci. Data*, 8, 297-323, <http://doi.org/10.5194/essd-8-297-2016>, 2016.
- Talley, L. D., Feely, R. A., Sloyan, B. M., Wanninkhof, R., Baringer, M. O., Bullister, J. L., Carlson, C. A., Doney, S. C., Fine, R. A., Firing, E., Gruber, N., Hansell, D. A., Ishii, M., Johnson, G. C., Katsumata, K., Key, R. M., Kramp, M., Langdon, C., Macdonald, A. M., Mathis, J. T., McDonagh, E. L., Mecking, S., Millero, F. J., Mordy, C. W., Nakano, T., Sabine, C. L., Smethie, W. M., Swift, J. H., Tanhua, T., Thurnherr, A. M., Warner, M. J., and Zhang, J.-Z.: Changes in ocean heat, carbon content, and ventilation: A review of the first decade of GO-SHIP global repeat hydrography, *Annu. Rev. Mar. Sci.*, 8, 185-215, <http://doi.org/10.1146/annurev-marine-052915-100829>, 2016.

203 Wang, X. T., Cohen, A. L., Luu, V., Ren, H., Su, Z., Haug, G. H., and Sigman, D. M.:
204 Natural forcing of the North Atlantic nitrogen cycle in the Anthropocene, Proc. Natl.
205 Acad. Sci., 115, 10606-10611, <http://doi.org/10.1073/pnas.1801049115>, 2018.

206 Woosley, R. J., Millero, F. J., and Wanninkhof, R.: Rapid anthropogenic changes in CO₂ and
207 pH in the Atlantic Ocean: 2003–2014, Global Biogeochem. Cycles, 30, 70-90,
208 <http://doi.org/10.1002/2015GB005248>, 2016.

209 Zhang, J.-Z., Mordy, C. W., Gordon, L. I., Ross, A., and Garcia, H. E.: Temporal trends in
210 deep ocean Redfield ratios, Science, 289, 1839-1839,
211 <http://doi.org/10.1126/science.289.5486.1839a>, 2000.

212